Improving the surface structure of high quality Sr_2FeMoO_6 thin films for multilayer structures.

I. Angervo[a,b,], M. Saloaro[a], J. Tikkanen[a,b], H. Huhtinen[a], P. Paturi[a]

[a] *Wihuri Physical Laboratory, Department of Physics and Astronomy, FI-20014 University of Turku, Finland*
[b] *University of Turku Graduate School (UTUGS), University of Turku, FI-20014 Turku, Finland*

Abstract

Two sets of Sr_2FeMoO_6 thin films were prepared with pulsed laser deposition and the effect of the laser fluence and the deposition temperature was investigated. The Sr_2FeMoO_6 thin films showed clear evidence of impurity phases when the laser fluence was altered. Phase pure films resulted through the whole temperature range between 900 °C and 1050 °C when a proper laser fluence was used. Films fabricated at lower deposition temperatures resulted with smaller surface roughnesses around 5 nm, higher Curie temperatures and with relatively high saturation magnetization values. The Curie temperature was determined from the minimum of the first order derivative and results showed the highest values of 350 K and above. The films with the highest Curie temperature reached zero magnetization above 400 K. The results indicate that both high microstructural and high magnetic quality Sr_2FeMoO_6 thin films can be obtained with a deposition temperature between 900 °C and 950 °C. This provides better fabrication parameters for the upcoming SFMO multilayer structures.

Keywords: SFMO, PLD, laser fluence, deposition temperature, roughness, Curie temperature

1. Introduction

The double perovskite Sr_2FeMoO_6 (SFMO) has been studied intensively in order to harness the material for future spintronic applications. Important

Email address: ijange@utu.fi (I. Angervo)

factors in SFMO considering the applications are 100% spin polarization and high Curie temperature (T_C), between $410 - 450$ K [1, 2]. However, the T_C, spin polarization as well as the saturation magnetization, M_{sat}, are strongly affected by structural imperfections like anti-site disorder (ASD) and oxygen vacancies [3, 4, 5, 6, 7, 8]. ASD refers to the misplacement of Fe and Mo ions in SFMO lattice structure, where the Fe has switched position with the Mo. Previous studies report a decrease in M_{sat} and/or T_C with an increase of ASD [4, 7, 9, 10]. Recent studies also report the increase of T_C and decrease of M_{sat} with increased oxygen vacancy concentration [9, 10].

Studies on SFMO are usually focused on polycrystalline samples or on smaller scale on SFMO thin film optimization, especially on the magnetic properties which have attracted great interest due to yet not well understood magnetic phenomena in SFMO thin films. All these studies provide important information, which help to understand the phenomena observed in SFMO, before the fabrication of SFMO spin valves. One of the key features in thin films is the film surface roughness which plays an important role in any thin film application, especially in multilayer devices, needed also in spin valves. The importance of flat interfaces in various multilayer systems has been reported in previous studies [11, 12]. Increased roughness between the layers in multilayer structures can lead to diminished exchange bias and magnetic coupling between layers [11, 12]. So far only a few studies have been published about SFMO multilayer structures [13, 14], which implies that more studies are needed for SFMO and especially for SFMO multilayer structures.

The main objective of this work is to find a path for improving the surface structure of SFMO thin films. Our previous study has shown some improvement in the surface roughness when the deposition temperature is decreased [15]. Here we have fabricated films with good structural and magnetic quality from a pulsed laser deposition (PLD) target synthesized by solid state reaction. Thin films simultaneously showed an improvement in the surface structure and in the T_C, both critical factors for the SFMO multilayer films, when the deposition temperature was decreased.

2. Experimental details

A ceramic SFMO PLD target was made by solid state synthesis. The ingredients for the synthesis, $SrCO_3$, Fe_2O_3 and MoO_3, were mixed using a mortar and the obtained fine mixture was compressed into a pellet. A calci-

nation was performed at 600 °C for 60 hours in ambient atmosphere. After the calcination the pellet was remortared, recompressed and then sintered at 1100 °C temperature for 24 hours in $Ar/5\%H_2$ atmosphere with additional H_2O gas. The chemical reaction, which takes place in the process, can be described with the formula

$$Fe_2O_3 + 4SrCO_3 + 2MoO_3 + H_2 \longrightarrow 2Sr_2FeMoO_6 + H_2O + 4CO_2. \quad (1)$$

To prevent the overreduction of the metal oxides into the respective elemental metals, the chemical balance was adjusted by introducing additional H_2O.

Two sets of SFMO thin films (hereafter: laser fluence L_f and temperature T_d), and one separate film named X1, were deposited on $SrTiO_3$ (100) single crystal substrates with PLD. The effects of laser fluence, L_f, and substrate deposition temperature, T_d, were investigated. The deposition parameters for the different films are shown in table 1. The films were deposited in a 9 Pa Ar-atmosphere with 2000 pulses. In addition one film with similar growth parameters to T4, but a pulse number of 500 was made to be used in the reflectivity measurements.

To determine the surface structure of the films, we used an Innova atomic force microscope (AFM) provided by Bruker. AFM measurements were done using the contact mode. The surface roughness was determined as the root mean square (RMS) roughness from 5×5 μm^2, 10×10 μm^2 and 20×20 μm^2 images. To check for possible impurity phases and to determine the c lattice parameter and 2θ full width of half maximum (FWHM) values $\theta - 2\theta$-scans between 20° and 110° were performed for polycrystalline SFMO and thin films, with a Philips X'Pert Pro MPD diffractometer with a Schulz goniometer. The texture $\phi - \psi$-scans of (204) peaks ($2\theta = 57.106°$) were measured for the texture analysis of SFMO films. We also measured the texture for the Fe (110) ($2\theta = 44.98°$) peak and the $SrMoO_4$ (112) ($2\theta = 27.68°$) peak for a more detailed impurity analysis of the thin films. A reflectivity measurement was carried out for a thinner film with 500 pulses in order to study the film thickness, since our XRD configuration is not capable of achieving a good reflectivity signal from the thicker films with 2000 pulses. The results indicate that 500 pulses correspond to 29 nm and the thickness of the 2000 pulse films were extrapolated assuming linear growth rate, which leads to a film thickness of 116 nm for the 2000 pulse films.

The magnetic properties of SFMO thin films were investigated with a Quantum Design MPMS SQUID magnetometer. Zero field cooled (ZFC) and

Table 1: PLD parameters for SFMO thin films.

SFMO thin film	Pulse number	L_f (J/cm^2)	T_d (°C)
L1	2000	1.59	1050
L2	2000	1.52	1050
L3/T1	2000	1.41	1050
L4	2000	1.30	1050
T2	2000	1.41	1000
T3	2000	1.41	950
T4	2000	1.41	900
X1	2000	1.59	900

field cooled (FC) temperature dependences of magnetization were measured between 10 K and 400 K in the field of 100 mT for the thin films. FC magnetization curve was used to determine the T_C from the minimum of the first order derivative. Hysteresis loops were measured between ±500 mT at temperatures of 10 K, 100 K, 300 K and 400 K. M_{sat} and the coercive field, B_c, were determined from the hysteresis loops measured at 10 K. The same measurements were also done for polycrystalline sample but due to their high T_C, in the polycrystalline sample and in some of the film samples, additional ZFC/FC measurements were done between 300 K and 500 K.

3. Results

3.1. Polycrystalline Sr_2FeMoO_6 target

The main focus of this paper is on SFMO thin films, but the results regarding the target used in the deposition are also briefly presented. Figure 1(a) shows the measured $\theta-2\theta$ scan (red) with the Rietveld refinement (blue) and the error line (black) between the measurement and the refinement for the polycrystalline SFMO target. The refinement was obtained with the Maud XRD-analysis program [16]. Only SFMO peaks are detected and we conlude that the SFMO target is phase pure within the limits of our XRD measurements, which are not able to detect possible impurity phases below 1% of total mass. The Rietveld refinement gives lattice parameters values

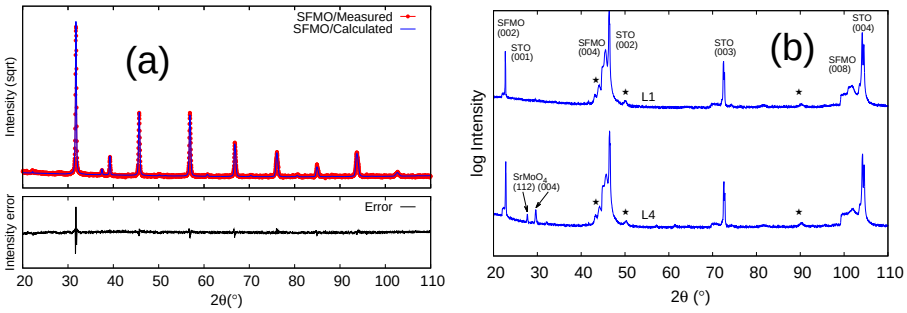

Figure 1: (a) $\theta - 2\theta$ scan (red) and Rietveld refienment (blue) performed for polycrystalline SFMO target. The "Error" line is the difference between measured and calculated intensity. (b) $\theta - 2\theta$ scans for L1 and L4 films. The results show SFMO and $SrTiO_3$ substrate $(00l)$ peaks, which are marked for L1 film. L4 also shows clear peaks, around 28° and 30°, arising most likely from $SrMoO_4$ impurity phase. Peaks near 44°, 51° and 90°, marked with $\star$, arise from the sample holder.

of $a = b = 5.569$ Å and $c = 7.896$ Å with a goodness of fit parameter $\chi = 1.68$. The values of the lattice parameters are quite close to the values reported in literature, $a = b = 5.575$ Å and $c = 7.893$ Å [17]. Magnetization versus temperature measurements of the polycrystalline sample showed a T_C of 408 K.

3.2. The effect of laser fluence

The first set of SFMO thin films was fabricated in order to study the effects of the laser fluence. The structural and the magnetic results for the first set are collectively presented in table 2. Figure 1(b) presents the $\theta - 2\theta$-results for L1 and L4. The $\theta - 2\theta$ scan for the L1 film shows only $(00l)$ peaks from SFMO, the $SrTiO_3$ substrate and the sample holder, as the $\theta - 2\theta$-scan of L3. However, the $\theta - 2\theta$-scan of the L4 reveals clear impurity peaks, which are also observed in the L2 film. The impurity peaks arise most likely from a $SrMoO_4$ phase, since the $\phi - \psi$-scans of $SrMoO_4$ also showed some texture. The nonmagnetic $SrMoO_4$ is a common impurity in polycrystalline SFMO and in SFMO thin films [18, 19, 20, 21]. No texture was observed in the other impurity pole figures of the other films, which together with $\theta - 2\theta$-scans indicate that the L1 and L3 films are phase pure. The impurity phase may have resulted from the changes in laser fluence. However, it is also possible that a phase separation in the target enables the formation of the

Table 2: The structural and magnetic results for the first set of SFMO thin films. The results show improvement in surface structure when using 1.41 J/cm^2 instead of 1.59 J/cm^2.

Sample	RMS (nm)	FWHM(008) (°)	c (Å)	T_C (K)	M_{sat} (μ_B/f.u.)	B_c (T)	$\frac{M(300\,K)}{M(10\,K)}$ (%)
L1	21.0	1.63	7.937	327	2.43	0.037	50/54
L2	27.2	2.15	7.926	348	1.53	0.037	57/62
L3/T1	12.5	0.55	7.936	322	2.36	0.022	41/42
L4	19.7	1.17	7.940	332	1.39	0.032	47/50

impurity phase. Although the target was shown to be phase pure, a small amount of a textured impurity phase below the XRD detection limit may exist in the target.

All of the films are c-axis oriented according to SFMO (204)-peak $\phi - \psi$ scans. The 2θ full width of half maximum (FWHM) was obtained for the SFMO (008)-peak by fitting the symmetric pseudo-Voigt profile. The SFMO (008)-peak is used instead of the higher intensity (004)-peak, because of a smaller overlap with the STO substrate peak. The L3 film has clearly the smallest 2θ-FWHM value of 0.55°, whereas the other films have values of 1.17° and over. The smaller 2θ-FWHM means smaller c-axis variation, which suggests a more homogenous structure and fewer structural defects, like stacking faults. We calculated the length of the c lattice parameter from the same fit. The $SrTiO_3$ (004) peaks were used as an internal standard. According to these results the c parameter values are between 7.926 Å and 7.940 Å This indicates less strain, which is expected due to the compressive inplane strain between the STO-substrate and the SFMO film, and more relaxed lattice parameter in L2 with the smallest c parameter value compared to the other films in the series. All the c-parameter values in the films are larger than the values in the polycrystalline samples, as has been reported here and elsewhere in the literature [17].

The AFM results show improvement in the surface structure of the L3 film, grown with 1.41 J/cm^2 laser fluence, compared to the other films. L3 has a surface roughness of 12.5 nm which is approximately 40% smaller than the roughness of L1, the only other pure film in the series. The 5×5 μm^2 AFM image is shown for L3 in the figure 3(a). All of the films, except for L1, appeared to have droplets on top of the smooth surface. This resembles

Stranski-Krastanov, single layer plus islands, growth. The L1 film had no smooth surface behind single droplets. Instead, the surface of L1 showed clusters of droplets without a smooth surface, which resembles Wolmer-Weber, 3D island, growth. However, the vertical scale of the surface structure is much larger than a single crystalline layer. The surface structure shows features of different growth modes but no clear evidence of single crystalline layer thin film growth.

The saturation magnetization determined from the 10 K hysteresis loop is rather high, 2.36 μ_B/f.u, for the L3 film. However, L1 has the highest M_{sat} of 2.43 μ_B/f.u and the M_{sat} values of the other two SFMO films are significantly lower. The lower M_{sat} values in L2 and L4 can be explained through the observed impurity. As a nonmagnetic material $SrMoO_4$ causes lower M_{sat} values in magnetic SFMO films, because it is impossible to reliably subtract the volume of the impurity phase from the total film volume. The $SrMoO_4$ phase could also induce Fe-rich SFMO with antiferromagnetically ordered (Fe-O-Fe) misorientation in the lattice structure. This would decrease the total magnetization even further [4, 7]. The coercive field, B_c, was defined as the average of the absolute values of the zero point of magnetization in a hysteresis loop measured at 10 K. The films with high B_c have also higher 2θ-FWHM values. Structural defects causing broadening in the XRD peaks can also cause domain wall pinning, resulting in higher B_c values [22].

The Curie temperature was determined as the minimum of the first order derivative of the FC-curve. L3 has the lowest T_C of 322 K and L2 has the highest T_C of 348 K. It appears that the films with a high T_C have a significantly lower M_{sat} than the films with a lower T_C. This could originate from higher oxygen vacancy concentration or lower antisite defect concentration. The oxygen vacancies have been shown to increase T_C and lower M_{sat}, whereas lower antisite defect concentration increases both the T_C and M_{sat} [7, 4, 9, 10]. This could mean that the films with the impurity phase have a rather good SFMO phase quality or a high oxygen vacancy concentration. However, the impurities could also directly affect to the magnetic interactions in SFMO causing changes in T_C. The fact that both M_{sat} and T_C are below the theoretical maximum values suggest defects like ASD and oxygen vacancies in some amount in all our SFMO thin films. Because the aim is to have room temperature applications, we determined the value of $M(300\,\mathrm{K})/M(10\,\mathrm{K})$, which provides information about the sample's usability at room temperature. $M(300,\mathrm{K})/M(10,\mathrm{K})$ was defined as the ratio of magnetization at 300 K to magnetization at 10 K. The $M(300\,\mathrm{K})/M(10\,\mathrm{K})$

values are higher in films with higher T_C, because 300 K is in the middle of ferro−paramagnetic transition in the films with lower T_C. With the highest T_C, L2 has the highest $M(300\,\mathrm{K})/M(10\,\mathrm{K})$ of 57%.

The objective was to improve the surface structure without diminishing other qualities. Eventhough L1 does have similar T_C and M_{sat} values to L3, the L3 with $L_f = 1.41\mathrm{J/cm}^2$, was chosen for further investigation due to the lower RMS roughness and the smaller 2θ-FWHM value. Other films were rejected because of high roughnesses and impurity phases.

3.3. The effect of deposition temperature

The L3 film was chosen as the basis of the T_d investigation and it was included in the second film set as T1. The XRD results for $\theta-2\theta$- and $\phi-\psi$-scans for the Fe(110) and $SrMoO_4$(112) show no impurities in any of these films. $2\theta-\theta$-scans for the second film set are similar to L1 in the figure 1(b). All of the films are also fully textured and c-axis oriented according to the SFMO (204)-peak $\phi-\psi$ scans. For a further structural characterization, the 2θ-FWHM values from SFMO (008) peaks are presented in the figure 2(a). The results show a decrease in the 2θ-FWHM values when T_d is increased above 900 °C, being constant above 900 °C temperature. This indicates a smaller variation in the c-axis in film with higher T_d values. The lattice parameter c was obtained from (008)-peaks and the results are shown in the figure 2(b). The c parameter has a maximum, 7.948 Å, with T_d of 1000 °C. Other c parameter values are above 7.937 Å. This would indicate more strain in the T2 film fabricated at 1000 °C. Again, all of the films have larger c parameter values than the value for our polycrystalline sample or the value reported in the literature [17]. The c parameter value of bulk SFMO appears as a dotted line in the figure 2(b) and clearly demonstrates that the changes in c parameter values between different films compared to the bulk value are only minor.

The 5×5 $\mu\mathrm{m}^2$ AFM images of the second SFMO thin film set are presented in the figure 3. Films appear to have droplets on their surface and a smooth background below the droplets. The size of the droplets seems to decrease when T_d decreases. The surface roughness as a function of T_d is presented in the figure 3(f). The roughness increases when T_d increases until the temperature of 1000 °C is reached. Above 1000 °C, the roughness decreases with temperature. Roughness values are smallest, around 5 nm, in the film deposited at 900 °C.

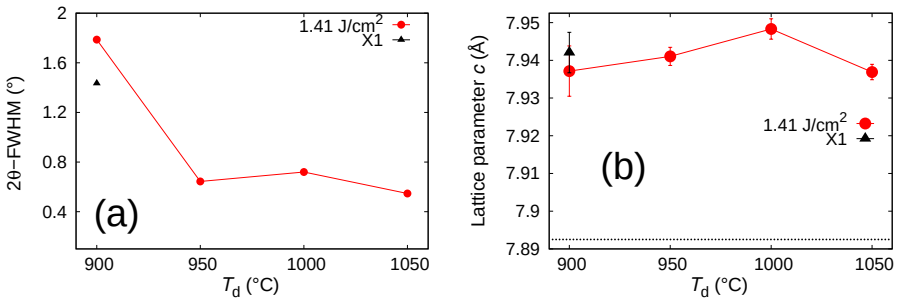

Figure 2: a) 2θ-FWHM presented as a function of T_{d}. 2θ-FWHM values are obtained from SFMO (008) peaks. b) lattice parameter c as a function of T_{d} with errorbars. The dotted line represents the bulk value of 7.893 Å as reported in the literature [17].

All of the films in the series showed evidence of Stranski-Krastanov-like growth as did most of the films in the L_{f} series. It seems however that the critical thickness for single layer growth is larger with a higher T_{d}. This results in the preferred smaller surface roughness in the films deposited at low T_{d}. However, the vertical scale of the surface structure is again much larger than a single crystalline layer. We have obtained similarly small roughness values for other SFMO thin films, which have have been accompanied with similar growth [23, 15]. Manako *et. al.* have reported step-and-terrace structures and spiral structures, which showed step sizes egual to 0.4 nm and 0.45 nm, respectively [24]. Other groups have also obtained similar AFM-images and/or smooth surface values for SFMO thin films fabricated at deposition temperatures below 950 °C [24, 25, 26, 27]. However, depending on the deposition parameters the magnetic properties appear to become worse with improved surface structure [15, 27, 26].

Improvement of the surface structure is important for the possible applications, but this should not be done at the expense of other structural and magnetic qualities. The ZFC/FC magnetization is presented as function of temperature in the figure 4(a) for L3/T1 and T4 SFMO thin films. The results are normalized by dividing the magnetization values with the (FC) magnetization value at 10 K temperature, $M_{\mathrm{FC}}(10\,\mathrm{K})$, for each film. The inset shows the first order derivatives of the FC curves from which the T_{C} was determined. It is clear from the figure 4(a), that the ferro−paramagnetic transition takes place at a significantly higher temperature in T4, deposited at 900 °C, compared to L3/T1, deposited at 1050 °C. The ferro−paramagnetic

transition is also sharper in T4. The ZFC- and FC-magnetizations show larger deviation at low temperatures in T4 and overall the deviations increased when T_{d} decreased.

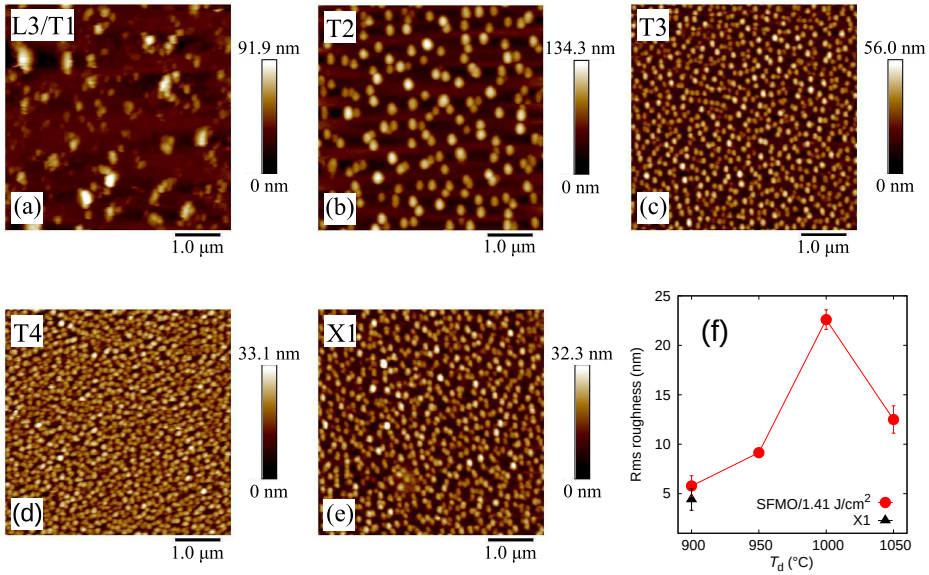

Figure 3: (a)-(e) 5×5 μm^2 size AFM images for the second set of SFMO thin films, where T_{d} is varied. (f) RMS roughness as a function of T_{d}. The measurement for the film thickness indicated the thickness value of 116 nm. The thickness is assumed equal in all our SFMO thin films.

T_{C} is presented as a function of T_{d} in the figure 4(b) (main panel). It can be clearly seen that the T_{C} increases when T_{d} decreases having the highest value, 350 °C, in T4 film deposited at 900 °C temperature. Our earlier results report the highest T_{C} for SFMO thin film around 380 K [28]. However, in this case T_{C} was determined from the first deviation point from the minimum magnetization, which resulted in higher values for T_{C}. If the same method was used here, the highest T_{C} value would be close to 400 K. As mentioned, ASD and oxygen vacancies affect the ferro−paramagnetic transition in SFMO. Higher T_{C} values are usually argued to be a result of lower ASD [4, 7], but an opposite tendency has been reported if ASD is below 10% [8]. Recent theoretical and experimental reports also show that higher oxygen vacancy concentration could increase the T_{C} [9, 10]. The results for T_{C} could

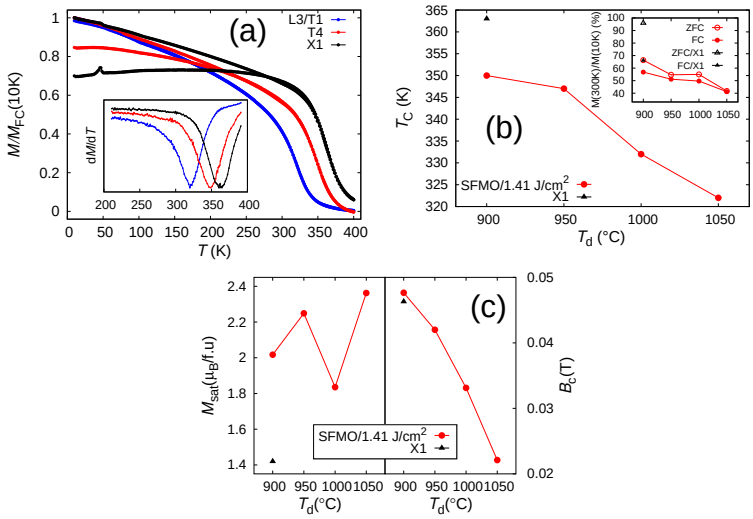

Figure 4: Normalized ZFC/FC magnetization vs temperature for L1, T4 and X1 films. Inset shows the first order derivative, used to define the Curie temperature, T_{C}, of the films. (b) The Curie temperature, T_{C}, as a function of T_{d} (main panel). The inset shows $M(300\,\mathrm{K})/M(10\,\mathrm{K})$ as a function of T_{d}. (c) The saturation magnetization, M_{sat}, (left) and the coercive field, B_{c}, (right) as functions of T_{d}.

indicate that film fabrication at lower T_{d} results in high quality SFMO or that the oxygen vacancy concentration increases at lower T_{d}.

Besides the high T_{C}, magnetization should be preserved at room temperature. Room temperature applications require a high spin polarization, which is related to the magnetization in SFMO at room temperature.
$M(300\,\mathrm{K})/M(10\,\mathrm{K})$ values are shown in the figure 4 (b) (inset) as a function of T_{d}. The results expectedly follow a tendency similar to that seen for T_{C}, since $M(300\,\mathrm{K})$ is in the middle of the ferro−paramagnetic transition of the SFMO film fabricated at 900 °C shows the highest $M(300\,\mathrm{K})/M(10\,\mathrm{K})$ values, over 55% for both FC and ZFC. This value is higher than the ones seen in the first SFMO thin film series, except for the value seen for L2. Since the high $M(300\,\mathrm{K})/M(10\,\mathrm{K})$ values are beneficial considering applications at room temperature, the T4 film fabricated at 900 °C shows the best potential for future studies.

The saturation magnetization, M_{sat}, as a function of T_{d} is presented in the left panel of the figure 4(c). Contrary to the T_{C}, the M_{sat} values show a

decrease when T_{d} decreases. L3/T1 has the highest M_{sat} value in the second film set, approximately 2.36 μ_{B}/f.u.. In the first series impurities played a major role in the M_{sat} results, which is not the case in this set. The M_{sat} values, even the highest value obtained here, are significantly lower than the theoretical maximum value of 4 μ_B/f.u. This implies magnetic distortion in the lattice structure, caused by ASD and oxygen vacancies, in all of our SFMO films in both of the film series. Theoretical and experimental studies report a decrease in M_{sat} with an increase of ASD and/or oxygen vacancy concentration [3, 4, 7, 8, 9, 10]. Combined with information from the T_{C} the results indicate a higher oxygen vacancy concentration in films deposited at 950 °C and below, causing the lower M_{sat} and the higher T_{C}. We acknowlegde that the M_{sat} values are also affected by the possible errors in the thin film volume. Changes in the growth parameters like L_{f} can affect the growth rate of the films, which here is assumed to be the same in all the films [29, 30]. Therefore, the comparison of the M_{sat} values between the two sets might not be reasonable. A higher laser fluence usually results in a higher deposition rate, up to a saturation [29, 30]. This would only increase the M_{sat} values obtained in the second SFMO film set, relative to the highest M_{sat} value obtained with L1 film of the first set.

The structural defects could also induce magnetic domain wall pinning in SFMO thin films [22]. Stronger domain wall pinning can be seen for example as a higher coercive field, B_{c}. The results for the B_{c} are presented in the right panel of the figure 4 (c). The B_{c} values decrease from 44 mT to 22 mT as T_{d} increases. Therefore, the T4 has a higher B_{c} compared to the other films, which suggests stronger domain wall pinning in T4. The AFM and XRD results indicate a higher defect concentration in the films fabricated at low T_{d}, which support this conclusion, because structural defects like grain boundaries, impurity phases, dislocations etc., cause domain wall pinning in magnetic systems. The larger deviation of the ZFC- and FC-magnetizations at low temperatures also results from stronger domain wall pinning. The larger deviation in T4 can be seen in the figure 4(a). The deviation decreased with increasing T_{d}.

Finally, we analyze the results for the X1 film. The X1 film was fabricated to verify the effects of L_{f} and T_{d} on the film's structural and magnetic properties. The deposition parameters L_{f} and T_{d}, were equal to the the parameters of L1 and T4, respectively. According to the XRD results, the X1 is phase pure, fully textured and c-axis oriented. 2θ-FWHM and c-parameter values, 1.5° and 7.939 Å, are quite close to the values obtained with T4. The

AFM-results in the figure 3(e) shows a surface with small droplets on top of a smooth background. The RMS roughness values (figure 3(f)) show improved surface roughness compared to the films fabricated at 1050 °C, approximately equal to 5 nm. The AFM results for X1 are similar to the results seen with T4. The magnetic results show that X1 actually has the highest T_{C} out of all of our SFMO films. The figure 4(a) and (b) clearly demonstrate that the ferro−paramagnetic transition is not even finished up to 400 K and the T_{C} is around 363 K. Additional $M(T)$ measurements up to the temperature of 500 K showed no ferromagnetic signal. Accordingly, the $M(300\,\mathrm{K})/M(10\,\mathrm{K})$ values are also highest in X1, but the ZFC- and FC-values also have the highest deviation. Even though the T_{C} is the largest in X1 the M_{sat} has the value of 1.41 μ_B/f.u, which is clearly the smallest value out of all of our phase pure films. The B_{c} value is also high in X1 but not quite the highest value compared to our other films as can be seen from the figure 4(c). Overall, the results for X1 are quite similar to T4 and no significant improvement was observed.

The final results indicate that an improved surface roughness can be best achieved with a lower T_{d} rather than controlling L_{f}. However, L_{f} might be critical for obtaining phase pure SFMO thin films. A lower T_{d} also results in a higher T_{C} and a smaller M_{sat}, both of which can explained through an increased oxygen vacancy concentration.

4. Conclusions

We have fabricated a phase pure polycrystalline SFMO PLD target using solid state synthesis. Two sets of SFMO thin films were fabricated with pulsed laser deposition and the effect of laser fluence and deposition temperature on the structural and magnetic properties were investigated. The goal was to find a way to improve the surface microstructure without diminishing other important factors. A $SrMoO_4$ impurity phase was observed with two different laser fluence values. With proper energy, phase pure *c*-axis oriented films were obtained through the whole applied temperature range between 900 °C and 1000 °C. When the deposition temperature was decreased the surface structure was improved and T_{C} was increased, but M_{sat} values showed a slight decrease with deposition temperature. Films fabricated at 900 °C had a smooth surface structure and a high T_{C}. Our results suggest that high quality SFMO thin films, with good structural and magnetic properties, can be achieved with T_{d} between 900 °C and 950 °C. However, 2θ-FWHM broaden-

ing and AFM results indicate a higher structural defect concentration, which could possibly enhance the magnetoresistive phenomenon but also diminish the zero field electrical transport properties.

Acknowledgments

This work was supported by the Jenny and Antti Wihuri foundation and the University of Turku Graduate School.

References

[1] K.-I. Kobayashi *et al.*, Nature **395**, 677 (1998).

[2] D. D. Sarma *et al.*, Phys. Rev. Lett. **85**, 2549 (2000).

[3] J. Navarro, J. Nogués, J. S. Muñoz ja J. Fontcuberta, Phys. Rev. B **67**, 174416 (2003).

[4] B. J. Park *et al.*, J. Magn. and Magn. Mater. **272-276**, 1851 (2004).

[5] D. Stoeffler ja S. Colis, J. Phys. Cond. Mat. **17**, 6415 (2005).

[6] D. Stoeffler ja S. Colis, J. Magn. and Magn. Mater. **290-291**, 400 (2005).

[7] A. S. Ogale, S. B. Ogale, R. Ramesh ja T. Venkatesan, Appl. Phys. Lett. **75**, 537 (1999).

[8] J. L. Alonso *et al.*, Phys. Rev. B **67**, 214423 (2003).

[9] M. Hoffmann *et al.*, arXiv:1504.02629 (2015).

[10] M. Saloaro *et al.*, ACS Applied Materials & Interfaces (submitted) (2015).

[11] A. Maitre, D. Ledue ja R. Patte, J. Magn. and Magn. Mater. **324**, 403 (2012).

[12] J. Kanak, T. Stobiecki ja S. Dijken, IEEE Transactions on Magnetics **44**, 238 (2008).

[13] D. Kumar ja D. Kaur, Materials Chemistry and Physics **129**, 802 (2011).

[14] D. Kumar ja D. Kaur, Journal of Alloys and Compounds **509**, 7886 (2011).

[15] P. Paturi, M. Metsänoja ja H. Huhtinen, Thin Solid Films **519**, 8047 (2011).

[16] L. Lutterotti, *Maud: Material Analysis Using Diffraction, Version 2.33* (http://maud.radiographema.com/, 1997).

[17] S. Nakamura ja K. Oikawa, J. Phys. Soc. Jpn. **72**, 3123 (2003).

[18] H. Deniz *et al.*, J. Mater. Sci. **50**, 3131 (2015).

[19] J. Santiso, A. Figueras ja J. Fraxedas, Surf. Interface Anal. **33**, 676 (2002).

[20] J. Raittila *et al.*, J. Phys. Chem. Solids **67**, 1712 (2006).

[21] X. H. Li *et al.*, Solid State. Commun. **145**, 98 (2008).

[22] D. Jiles ja D. Atherton, Journal of Magnetism and Magnetic Materials **61**, 48 (1986).

[23] T. Suominen, J. Raittila ja P. Paturi, Thin Solid Films **517**, 5793 (2009).

[24] T. Manako *et al.*, Appl. Phys. Lett. **74**, 2215 (1999).

[25] H. Jalili, N. F. Heinig ja K. T. Leung, J. Chem. Phys **132**, 204701 (2010).

[26] R. P. Borges *et al.*, Thin Solid Films **429**, 5 (2003).

[27] D. Kumar ja D. Kaur, Physica B **405**, 3259 (2010).

[28] M. Saloaro, S. Majumdar, H. Huhtinen ja P. Paturi, EPJ Web of Conferences **40**, 15012 (2013).

[29] H. U. Krebs, International Journal of Non-Equilibrium Processing **10**, 3 (1997).

[30] J. Brandenburg *et al.*, Applied Physics A **79**, 1005 (2004).